Inorg. Chem. **2008**, *47*, 7211−7224

Solid State and Aqueous Solution Characterization of Rectangular Tetranuclear $V^{IV/V}$-*p*-Semiquinonate/Hydroquinonate Complexes Exhibiting a Proton Induced Electron Transfer

Chryssoula Drouza[†] and Anastasios D. Keramidas*[,‡]

Department of Agriculture Production, Biotechnology and Food Science, Cyprus University of Technology, 3603 Limasol, Cyprus, and Department of Chemistry, University of Cyprus, 1678 Nicosia, Cyprus

Received March 31, 2008

Reaction of the non-innocent dinucleating ligand 2,5-bis[N,N-bis(carboxymethyl) aminomethyl]hydroquinone (H_6bicah) with VO^{2+} and VO_4^{3-} salts in water in the pH range 2 to 4.5 provides a series of novel tetranuclear V^{IV} and/or V^{V} macrocycles with the main core consisting of the anions $[V^{V}_4O_4(\mu\text{-}O)_2(\mu\text{-bicah})_2]^{4-}$ isolated at pH = 2.5 and $[V^{IV}_2V^{V}_2O_4(\mu\text{-}O)_2(\mu\text{-bicas})(\mu\text{-bicah})]^{5-}$ and $[V^{IV}_4O_4(\mu\text{-}O)_2(\mu\text{-bicas})_2]^{6-}$ isolated at pH = 4.5 (bicas$^{\bullet 5-}$ = 2,5-bis[N,N-bis(carboxymethyl) aminomethyl]-*p*-semiquinonate), whereas at pH = 2 the dinuclear $[(V^{IV}O)_2(OH_2)_2(\mu\text{-bicah})]^{2-}$ was obtained. All vanadium compounds have been characterized, and the charge of the ligand has been assigned in solid state by X-ray crystallography and infrared spectroscopy. The structures of the tetranuclear anions consist of four vanadium atoms arranged at the corners of a rectangle with the two bridging bicas$^{\bullet 5-}$ and/or bicah^{6-} ligands on the long and the two $V^{IV/V}-O-V^{IV/V}$ bridges on the short sides of the rectangle. UV−vis, ^{51}V and ^{1}H NMR spectroscopy and electrochemistry showed that these complexes interconvert to each other by varying the pH. This pH induced redox transformation of the tetranuclear anions has been attributed to the shift of the reduction potential of the bicas$^{\bullet 5-}$ to higher values by decreasing the pH. The electron is transferred intramolecularly from the metal ion to the electron accepting semiquinones resulting in reduction of bicas$^{\bullet 5-}$ to bicah^{6-} and concurrent oxidation of the V^{IV} to V^{V}. The resulting complexes are further oxidized by atmospheric oxygen. This system as a model for the H^+ coupled redox reactions in metalloenzymes and its relevance is discussed briefly.

Introduction

The three redox species of the hydroquinone and hydroquinone derivatives, hydroquinone, *p*-semiquinone, and *p*-quinone, are important proton/electron sources and sinks that play an essential role in electron/proton coupled biochemical processes.[1,2] For example, electron transfer reactions between transition metal centers and *p*-quinone cofactors are vital for all life, occurring in key biological processes as diverse as the oxidative maintenance of biological amine levels,[3,4] tissue (collagen and elastin) formation,[4–6] photosynthesis,[7,8] and aerobic (mitochondrial) respiration.[9,10] The metal ions in these systems lie in close proximity to *p*-semiquinone radicals resulting in immediate interaction. In the Photosystem II (PSII) reaction center, for example, a plastoquinone-9 (Q_A, a substituted *p*-quinone) is magnetically coupled with a non heme high spin iron(II) ion when it is reduced to the long

* To whom correspondence should be addressed. E-mail: akeramid@ucy.ac.cy.
† Cyprus University of Technology.
‡ University of Cyprus.

(1) Rappoport, Z. *The Chemistry of the Quinoid Compounds*; Wiley: New York, 1988; Vols. *1 and 2*.
(2) Yano, T.; Magnitsky, S.; Ohnishi, T. *Biochim. Biophys. Acta-Bioenerg.* **2000**, *1459*, 299.
(3) Dooley, D. M.; Scott, R. A.; Knowles, P. F.; Colangelo, C. M.; McGuirl, M. A.; Brown, D. E. *J. Am. Chem. Soc.* **1998**, *120*, 2599.
(4) Klinman, J. P. *Chem. Rev.* **1996**, *96*, 2541.
(5) McIntire, W. S. *Annu. Rev. Nutr.* **1998**, *18*, 145.
(6) Wang, S. X.; Mure, M.; Medzihradsky, K. F.; Burlingame, A. L.; Brown, D. E.; Dooley, D. M.; Smith, A. J.; Kagan, H. M.; Klinman, J. P. *Science* **1996**, *273*, 1076.
(7) Calvo, R.; Abrecsch, E. C.; Bittl, R.; Feher, G.; Hofbauer, W.; Isaacson, R. A.; Lubitz, W.; Okamura, M. Y.; Paddock, M. *J. Am. Chem. Soc.* **2000**, *122*, 7327.
(8) Hoganson, C. W.; Babcock, G. T. *Science* **1997**, *277*, 1953.
(9) Nichols, D. G.; Ferguson, S. J. *Bioenergetics 2*; Academic Press: New York, 1992.
(10) Iwata, S.; Lee, L. W.; Okada, K.; Lee, J. K.; Iwata, M.; Rasmussen, B.; Link, T. A.; Ramaswamy, S.; Jap, B. K. *Science* **1998**, *281*, 64.

10.1021/ic800569t CCC: $40.75
Published on Web 07/19/2008

time stable semiquinone radical.[11] The magnetic properties of the Q_A site are dependent on the environment of quinone, mainly hydrogen bonds with the neighbor hydrogen bearing nitrogen groups, which are controlled by the pH.[12] In another example, the proposed catalytic cycle in copper amine oxidases (CAOs) involves the intermediate reduced state of the enzyme (E_{red}) containing aminoquinol (TPQ_{red}) and a cupric ion in equilibrium with the form of the enzyme whose proton and electron transfer lead to a cuprous ion and an iminosemiquinone (TPQ_{sq}).[13]

Although the crystal structures of many of these enzymes have been solved, the role of the metal ions in these reactions has still been controversial. The investigation of the association between the electron and the proton transfer in the metal ion −hydroquinone/semiquinone/quinone interacting systems is particularly important to understand the factors which regulate the redox potentials and the pathways in electron transfer reactions between transition metal centers and *p*-semiquinone radicals. To explore and elucidate the intrinsic chemistry of the active site of these metalloproteins, we pursue studies on smaller model complexes.

Covalently bonded molecules of strong oxidizing metal ions with hydroquinones can provide unique well-defined model systems to probe the mechanisms of the proton-coupled electron transfer reactions, since the metal centered and the ligand redox potentials are similar and the redox potential of the quinonoid compound can be readily controlled by protonation[14,15] and solvation.[16] From an other point of view, the controlled quinonoid in these complexes might behave as a pH sensitive redox switch. Thus, beyond providing an insight into biosystems, information of this kind will underpin key technological advances in the areas of batteries, sensors, and "smart" materials for triggered drug release applications.[17–19] In marked contrast to the extensive structural chemistry for chelate stabilized *o*-(hydro/semi-)quinone metal compounds,[20–28] examples of structurally characterized σ-bonded *p*-hydroquinone-metal complexes[29,30] are surprisingly rare, and there is only one example of σ-bonded *p*-semiquinone-metal molecule reported by our group.[31] This is mainly due to the absence of a chelate coordination site in simple *p*-(hydro/semi)quinone. A strategy to prepare such species is to synthesize substituted *p*-hydroquinones in *o*-position with substituents containing one or more donor atoms, thus, enabling the metal atom to form chelate rings. Amino and carboxylate substituents satisfy the requirement for proton accepting groups and an environment around metal ions redox coupled with quinone similar to that found in natural systems. Thus, such molecules represent very good models in biomimetic studies of protein active centers. The introduction of amino-carboxylate groups at the *o*-position in phenols may serve as proton-accepting sites in concerted proton−electron transfer reactions.[14,32]

In a previous communication we have reported that reaction of V^{IV} and V^{V} with the disubstituted *p*-hydroquinone ligand, 5-bis[N,N-bis(carboxymethyl)aminomethyl]hydroquinonate ($bicah^{6-}$), resulted in the synthesis of the first structurally characterized tetranuclear σ-bonded vanadium(IV)−bis(*p*-semiquinonate) complex.[31] The spontaneous transfer of one electron from the ligand to the metal center, as well the theoretical study,[31] show that the difference between the lowest half-occupied molecular orbital centered on the metal ion and the highest molecular orbital centered on the semiquinone ligand is small. The oxidative ability of the ligand can be controlled by varying the pH, and thus, this complex provides an ideal model sensitive to pH for studying the intramolecular electron transfer between the *p*-semiquinone and the metal ion. In addition, the free *p*-semiquinones are not stable in aqueous or protic solvents, as this is observed by the electrochemistry of *p*-quinones which are reduced by a two electron process directly to hydroquinones.[15] In contrast, the unique stabilization of the *p*-semiquinonate radicals in aqueous solution by ligation to vanadium ions serves as a model for the enzymes that operate via a *p*-semiquinone radical, acting in one electron transfer reactions. The rich redox chemistry of vanadium, exhibiting high stability in the three different oxidation states III, IV, and V in aqueous solution, is well suited for such investigation because of the versatility of vanadium to act reversibly as electron donor and acceptor. The interaction of *p*-hydroquinones with vanadium in high-oxidation states presents additional interest because of the participation of vanadium in redox reactions in biological systems[33] such as the reduction of vanadium(V), present in seawater, to vanadium(III) in the blood cells of tunicates.[34,35]

Our focus in this work is on the synthesis and characterization in solid state and solution of stable complexes of

(11) Kilimov, V. V.; Dolan, E.; Shaw, E. R.; Ke, B. *Proc. Natl. Acad. Sci. U.S.A.* **1980**, *77*, 7227.
(12) Deligiannakis, Y.; Hanley, J.; Rutherford, W. A. *J. Am. Chem. Soc.* **1999**, *212*, 7653.
(13) Mure, M. *Acc. Chem. Res.* **2004**, *37*, 131.
(14) Costentin, C.; Robert, M.; Saveant, J.-M. *J. Am. Chem. Soc.* **2006**, *128*, 8726.
(15) Lehman, M. W.; Evans, D. H. *J. Phys. Chem. B* **2001**, *105*, 8877.
(16) Gupta, N.; Linschitz, H. *J. Am. Chem. Soc.* **1997**, *119*, 6384.
(17) Evangelio, E.; Ruiz-Molina, D. *Eur. J. Inorg. Chem.* **2005**, 2975.
(18) Fabbrizzi, L.; Licchelli, M.; Pallavicini, P. *Acc. Chem. Res.* **1999**, *32*, 846.
(19) Dei, A.; Gatteschi, D.; Sangregorio, C.; Sorace, L. *Acc. Chem. Res.* **2004**, *37*, 827.
(20) Pierpont, C. G. *Inorg. Chem.* **2001**, *40*, 5727.
(21) Pierpont, C. G. *Coord. Chem. Rev.* **2001**, *99*, 2019.
(22) Pierpont, C. G. *Coord. Chem. Rev.* **2001**, *99*, 216–217.
(23) Pierpont, C. G. *Coord. Chem. Rev.* **2001**, *21*, 9221, 415.
(24) Pierpont, C. G.; Lange, C. *Prog. Inorg. Chem.* **1994**, *41*, 331.
(25) Pierpont, C. G.; Lange, C. W. *Progr. Coord. Chem.* **1993**, *41*, 381.
(26) Adams, D. M.; Rheingold, A. L.; Hendrickson, D. N. *J. Am. Chem. Soc.* **1993**, *115*, 8221.
(27) Adams, D. M.; Hendrickson, D. N. *J. Am. Chem. Soc.* **1996**, *118*, 11515.
(28) Jung, O. S.; Jo, D. H.; Lee, Y. A.; Conklin, B. J.; Pierpont, C. G. *Inorg. Chem.* **1997**, *36*, 19.
(29) Tanski, J. M.; Wolczanski, P. T. *Inorg. Chem.* **2001**, *40*, 346.
(30) Vaid, T. P.; Lobkovsky, E. B.; Wolczanski, P. T. *Inorg. Chem.* **2001**, *40*, 346.
(31) Drouza, C.; Tolis, V.; Gramlich, V.; Raptopoulou, C.; Terzis, A.; Sigalas, M. P.; Kabanos, T. A.; Keramidas, A. D. *Chem. Commun.* **2002**, 2786.
(32) Costentin, C.; Robert, M.; Saveant, J.-M. *J. Am. Chem. Soc.* **2006**, *128*, 4552.
(33) Rehder, D. *Coord. Chem. Rev.* **1999**, *182*, 197; the coordination chemistry of vanadium as related to its biological functions.
(34) Frank, P.; Hodgson, K. O. *Inorg. Chem.* **2000**, *39*, 6018.
(35) Michibata, H.; Sakurai, H., In *Vanadium in Biological Systems*; Chasteen, N. D., Ed.; Kluer Academic Publishers: Dordrecht, 1990; pp 153−171.

vanadium with *p*-semiquinonate radicals, as well as the investigation of the H^+ induced electron transfer between the V^{IV}/V^V metal centers and the coordinated semiquinonate/hydroquinonate ligands. The V^{IV}/V^V−semiquinonate/hydroquinonate tetranuclear species produced from this electron transfer were isolated from aqueous solution, and the oxidation states of the ligand were indisputably determined by X-ray crystallography. UV−vis and NMR spectroscopies and electrochemistry were employed for the investigation of the H^+ induced redox reaction in aqueous solution.

Experimental Section

Materials and Methods. Materials. Sodium metavanadate, vanadium pentoxide, vanadyl sulfate, iminodiacetic acid, 1,4-hydroquinone, and guanidine carbonate were purchased from Aldrich. Ammonium metavanadate and sodium hydroxide were purchased from Scharlau, paraformaldehyde from GPR. All chemicals and organic solvents were used without further purification. Stock solution of vanadyl chloride 0.920 M was prepared as follows: Vanadyl sulfate (10.0 g, 46.0 mmol) was placed in a beaker with 50 mL of water and $BaCl_2$ (13.0 g, 62.0 mmol) was added under stirring. The formed white precipitate was filtrated. The filtrate was evaporated till dry, then ethanol (1 mL) and acetonitrile (20 mL) were added. The blue solution was filtrated, and the filtrate was evaporated till dry. Acetonitrile was added to dissolve the green residue and transferred to a 50.0 mL volumetric flask, which was filled with acetonitrile. A stock solution of guanidinium vanadate (0.250 M) was prepared by mixing vanadium pentoxide (2.27 g, 0.0125 mol) with guanidine carbonate (6.85 g, 0.0125 mol) and water (70 mL). The mixture was stirred and heated until a clear yellow solution was formed. The total volume of the solution was adjusted at 100.0 mL by addition of water. Stock solution of potassium vanadate (0.250 M) was prepared by slow addition of potassium hydroxide (3.5 g, 0.063 mol) to a suspension of vanadium pentoxide (5.68 g, 0.0312 mol) in 150 mL of water, under stirring. The volume of the resultant clear colorless solution was adjusted to 250.0 mL by addition of water. Complexes **7** and **8** are referred to the compounds $\{Na_6[(VO)_2(\mu\text{-}O)(\mu\text{-bicas})]_2\}\cdot Na_2SO_4\cdot 20H_2O$ and $\{Na_4[(VO_2)_2(\mu\text{-bicah})]\}\cdot 2H_2O$ respectively in ref 31. $Guan^+$ is the abbreviation for the guanidine cation. The syntheses of all vanadium complexes were performed under Ar atmosphere up to final pH adjustment to avoid aerial oxidation and formation of green colored byproducts.

Synthesis of H_6bicah·$2H_2O$. Iminodiacetic acid (10.0 g, 75.0 mmol) was placed in a 100 mL round two neck flask together with paraformaldehyde (2.48 g, 82.6 mmol), 8 mL of water and 2 mL of ethanol. The mixture was stirred and intensively bubbled with Ar for 20 min. Sodium hydroxide (6.00 g, 150 mmol) plus 2 mL of ethanol were added resulting in a yellowish solution. 1,4-Hydroquinone (4.14 g, 0.0376 mol) was added to the above solution under Ar, and the color of the solution turned to dark red. The solution was refluxed for 6 h under an Ar atmosphere. During the reflux, a white precipitate was formed. The mixture was cooled down at room temperature under nitrogen, and the pH was adjusted at 2.7 by 6 M HCl. The mixture was cooled at 4 °C overnight and was suction filtrated. The solid was rinsed with 2 × 3 mL of slightly acidified cold water and 1 × 2 mL of ethanol and dried under vacuum. The yield of H_6bicah was 80% based on hydroquinone. Anal. Calcd for $C_{16}H_{24}N_2O_{12}$: C, 44.04; H, 5.54; N, 6.42. Found: C, 43.89; H, 5.63; N, 6.31. IR (KBr, cm^{-1}): $\nu(C-O_{hydroquinonate})$ 1203.

Synthesis of $Guan_2[V^{IV}_2O_2(OH_2)_2(\mu\text{-bicah})]\cdot 7H_2O$ (1), $Guan_4[V^V_4O_4(\mu\text{-}O)_2(\mu\text{-bicah})_2]\cdot(CH_3)_2CO\cdot 2H_2O$ (2), and $Guan_5[V^{IV}_2V^V_2O_4(\mu\text{-}O)_2(\mu\text{-bicas})(\mu\text{-bicah})]\cdot 2C_2H_5OH\cdot 12H_2O$ (4). H_6bicah (0.500 g, 1.18 mmol) was mixed with vanadyl chloride (1.29 mL of 0.920 M freshly prepared acetonitrile solution, 1.19 mmol) resulting in a light blue suspension. Guanidine vanadate (4.73 mL of 0.250 M water solution, 1.18 mmol) was added to the above mixture. The color turned to dark violet, and the pH of the solution was 4.83. The solution was filtrated, diluted by adding water equal to the volume of the solution, and separated to two equal aliquots. Ethanol was slowly diffused (4−5 months) into the first aliquot at 4 °C giving dark blue crystals of **4** suitable for X-ray analysis. The yield was 90%. The pH of the second aliquot was adjusted at 2.8 with 3 M HCl. The solution was left to slowly evaporate at 4 °C for 3−4 months. Dark blue monocrystals of **2** and few light green-blue monocrystals of **1** suitable for X-ray diffraction analysis were coprecipitated during evaporation; these were separated by hand and analyzed. The yield in **2** was 85%. Anal. Calcd for **1**, $C_{18}H_{44}N_8O_{21}V_2$: C, 26.68; H, 5.47; N, 13.83, Found: C, 26.41; H, 5.55; N, 13.74. Anal. Calcd for **2**, $C_{42}H_{72}N_{16}O_{32}V_4$: C, 33.26; H, 4.78; N, 14.77, Found: C, 33.42; H, 4.51; N, 14.89. Anal. Calcd for **4**, $C_{41}H_{94}N_{19}O_{40}V_4$: C, 29.02; H, 5.58; N, 15.68. Found: C, 28.84; H, 5.72; N, 15.53.

Synthesis of $Guan_3Na[V^V_4O_4(\mu\text{-}O)_2(\mu\text{-bicah})_2]\cdot C_2H_5OH\cdot 7H_2O$ (3) and 2. A suspension of H_6bicah (1.00 g, 2.36 mmol) in H_2O (4 mL) was dissolved with the addition of 3 M sodium hydroxide at pH 5. Sodium metavanadate (0.300 g, 2.46 mmol) dissolved in 1−2 mL of hot water was added. The color of the solution turned from yellowish to red, and the pH was increased to 8.7. Vanadyl sulfate (0.530 g, 2.44 mmol) dissolved in 2 mL of water was added to the above solution. The color turned to dark blue, and the pH was decreased to 4.8. The mixture was stirred for 15 min, and the pH was fixed at 2.5 by addition of 5 M HCl. The solution was filtrated, ethanol was added until it became cloudy, and placed in a refrigerator. One week later, a dark blue precipitate was formed and the mixture was filtrated, rinsed with ethanol (1 × 2 mL), and dried under vacuum. A quantity of the isolated compound (0.10 g) was dissolved in water (4−5 mL) and in the solution guanidine carbonate (0.10 g, 0.55 mmol) was added gradually, keeping the pH of the solution at 2.8 with concurrent addition of 6 M HCl. Dark blue-violet crystals of **3** suitable for X-rays analysis were obtained by slow diffusion of ethanol into this solution at 4 °C. The total yield was 35%. Diffusion of ethanol into the above solutions diluted by 4−5 mL water resulted in the crystallization of **2** instead of **3**. Anal. Calcd for **3**, $C_{37}H_{66}N_{13}NaO_{34}V_4$: C, 30.36; H, 4.54; N, 12.44. Found: C, 29.98; H, 4.63; N, 12.39. IR (KBr, cm^{-1}): $\nu(C-O_{hydroquinonate})$ 1286, 1145.

Synthesis of $Guan_3NaK[V^{IV}_2V^V_2O_4(\mu\text{-}O)_2(\mu\text{-bicas})(\mu\text{-bicah})]\cdot 2CH_3OH\cdot 7H_2O$ (5) and 2. A solution of vanadyl sulfate (0.260 g, 1.20 mmol) in water (2 mL) was added to a suspension of H_6bicah (0.500 g, 1.18 mmol) in water (3 mL). Potassium vanadate (4.30 mL of 0.275 M aqueous solution, 1.18 mmol) was added to the above mixture under stirring (pH = 4.90) resulting in a dark blue solution. Subsequently guanidine carbonate (1.06 g, 5.88 mmol solution in 3 mL of water acidified at pH 4 using 6 M HCl) was added, and the final solution (pH = 4.80) was filtrated and separated into 2 aliquots. Methanol was slowly diffused (4−5 months) into the first aliquot at 4 °C resulting in precipitation of monocrystals of **5** suitable for X-rays analysis. The yield was 65%. Anal. Calcd for **5**, $C_{37}H_{68}KN_{13}NaO_{35}V_4$: C, 29.22; H, 4.51; N, 11.97. Found: C, 28.93; H, 4.69; N, 11.78.

The second aliquot was treated with 3 M HCl to adjust the pH at 2.7. Diffusion of ethanol into these samples at 4 °C resulted in the formation of monocrystals of **2**.

Synthesis of $Na_4(NH_4^+)_2[V^{IV}_4O_4(\mu\text{-}O)_2(\mu\text{-bicas})_2]\cdot 2CH_3OH\cdot 13H_2O$ (6). Vanadyl chloride (1.36 mL of a 0.920 M acetonitrile solution, 1.25 mmol) was added to a suspension of H_6bicah (0.550 g, 1.30 mmol) in water (3 mL). Under stirring, ammonium metavanadate (0.140 g, 1.25 mmol) dissolved in 1−2 mL of water, and NaCl (0.096 g, 1.5 mmol) was added to the above suspension resulting in the formation of a dark blue-violet solution (pH = 5.00). Stirring was continued for 15 min, and the mixture was filtrated. Single crystals of **6**, appropriate for X-ray diffraction structure determination, were obtained by slow diffusion of methanol into the above solution. The yield was 45%. Anal. Calcd for **5**, $C_{34}H_{70}KN_6Na_4O_{41}V_4$: C, 26.96; H, 4.66; N, 5.55. Found: C, 26.79; H, 4.78; N, 5.44. UV−vis {H_2O, pH=4.8, λ(nm) [ε (M^{-1} cm^{-1})]}: 856 [8000] ($\pi_{Semiquinonate}\rightarrow d\pi$); 625 [9300] ($\pi_{Semiquinonate}\rightarrow d\sigma$); 295(sh) [10300] ($\pi$-$\pi^*$, semiquinonate).

Synthesis of 7′ Complex **7**[31] (0.10 g) was dissolved in water (4−5 mL) resulting in the formation of a dark blue solution (pH = 4.5). The pH of the solution was adjusted at 2.8 with the addition 6 M HCl. A dark blue solid of **7′** (0.11 g) was obtained by slow diffusion of ethanol into this solution at 4 °C. Together with **7′**, white Na_2SO_4 had been coprecipitated which it was not possible to separate from the bulk material. However, the molecule was characterized by ^{51}V, ^{1}H NMR, UV−vis and IR spectroscopies, and it was found to exhibit spectra similar to **2** and **3** indicating that the tetranuclear anion is identical in these complexes. UV−vis {H_2O, pH=4.8, λ(nm) [ε ($M^{-1}cm^{-1}$)]}: 780 [23000] ($\pi_{hydroquinonate}\rightarrow d\pi$); 642(sh) [10300] ($\pi_{hydroquinonate}\rightarrow d\sigma$); 317 [23000] ($\pi$-$\pi^*$, hydroquinonate); 260(sh) [29000].

X-ray Studies. Single crystal analysis was performed on an Xcalibur Oxford Difractometer equipped with a Sapphire 3 CCD detector and a 4-cycle Kappa geometry goniometer, using enhanced Mo Kα (λ=0.7107 Å) X-ray source and graphite radiation monochromator. An analytical absorption correction was applied using CrysAlis RED software. CrysAlis CCD and CrysAlis RED softwares were used for data collection and data reduction/cell refinement, respectively.[36,37] The structure of the compounds was solved by direct methods and refined by full-matrix least-squares techniques on F^2 by using SHELXS-97.[38,39] Special computing molecular graphics incorporated in the WinGX 3.2 interface were used.[40] Experimental data for this study are listed in Table 1. All the non-H atoms were refined anisotropically. The positions of hydrogen atoms of **1**−**6** were calculated from stereochemical considerations and kept fixed isotropic during refinement or found in a DF map and refined with isotropic thermal parameters.

NMR and Magnetic Measurements. All NMR samples were prepared from crystalline compounds in D_2O at room temperature immediately before NMR spectrometric determinations. All samples used for NMR measurements were prepared in triplicate, typically at concentrations of 4.8 to 9.2 mM complex, and DCl (1 M) was used to lower pH at 3.0. NMR spectra were recorded on a Bruker Avance 300 spectrometer at 300 MHz for ^{1}H and 78.9 MHz for ^{51}V NMR. A 30°-pulse width was applied for both the ^{1}H and ^{51}V NMR spectra, which were acquired with a 3000 and 30000 Hz spectral window, and a 1 and 0.001 s relaxation delay, respectively. Magnetic measurements were carried out on an MK1 MB magnetic susceptibility balance.

UV−vis and IR Measurements. The samples for UV−vis studies were aqueous solutions prepared from crystalline compounds and KCl to keep ionic strength constant at 0.1 M. The stability of the compounds was examined over the concentration range of 6 to 150 μM, and the time dependence measurements were determined at typical concentrations of 66 to 86 μM complex. The spectra were recorded on a Photonics UV−vis spectrophotometer Model 400, equipped with a CCD array, operating in the range 200 to 900 nm.

IR spectra were recorded on a Jasco FT-IR 460 Plus spectrometer in KBr pellets, and microanalyses were conducted on a Eurovector 3000 Elemental Analyzer.

Electrochemistry. Cyclic voltammetry (CV) and round disk voltammetry (RDV) experiments were recorded using an EG&G Princeton Applied Research 273A potentiostat/galvanostat. Electrochemical procedures were performed with a three-electrode configuration: a platinum disk or rotating disk electrode (RDE) was used as the working electrode, a platinum wire as the auxiliary electrode, and a $Hg/HgSO_4$ electrode as reference. All the potential values are referred to the normal hydrogen electrode (NHE). The electrochemical measurements were carried out in water solutions of KNO_3 (0.2 M) purged with N_2 prior to the measurement at 298 K. Scan rates (ν) of 100 mV s^{-1} and 10 mV s^{-1} were used for CVs and linear sweep voltammetry experiments, respectively. The working electrode was cleaned after every run because depositions on the surface of the electrodes alter the peaks in the voltammograms. In the exhaustive electrolysis/coulometric experiments, the working electrode was replaced with a platinum 52 mesh gauze electrode, and the auxiliary electrode was separated from the bulk solution by a fritted disk.

A solution of 0.10 M $CH_3COOH-CH_3COO^-Na^+$ was used as buffer in the electrochemistry experiments in which the pH was kept constant at 4.5 and 3.0.

Sample Preparation. All solutions were prepared by dissolution of crystals of complexes whose purity was examined optically under the microscope, and a few of them were examined in the X-ray diffractometer to ensure that only the desired redox isomer was present in the sample. All the experiments were repeated more than three times to ensure the repeatability of the results. The water used for the experiments under Ar was boiled for 20 min under continued bubbling with Ar and cooled at ambient temperature prior to use.

To simplify the discussion, we used the following terminology for the different tetranuclear cores: each tetranuclear core is noted as XX^{n-} with $n = 4$, 5, or 6 being the total charge of the tetranuclear core, while X refers to the oxidation of the ligand, H for hydroquinone, and S for semiquinone. For example, complexes **6** and **7**, which contain two semiquinones and the tetranuclear core has total charge −6, are referred as SS^{6-}.

Results and Discussion

Syntheses of the Compounds. The organic hydroquinone ligand H_6bicah was synthesized using the Mannich reaction.[41] In this synthesis, 1 equiv of hydroquinone, 2 equiv of formaldehyde, and iminodiacetic acid were allowed to react in water−ethanol solution at alkaline pH. This alkaline solution is very sensitive toward oxidation of hydroquinone.

(36) *CrysAlis CCD*, 1.171.29.9; Oxford Diffraction Ltd.: Abingdon, U.K., 2006.
(37) *CrysAlis RED*, 1.171.29.9;Oxford Diffraction Ltd.: Abingdon, U.K., 2006.
(38) Sheldrick, G. M., *SHELXS-97: Program for the Solution of Crystal Structure*; University of Göttingen: Göttingen, Germany, 1997.
(39) Sheldrick, G. M., *SHELXL-97: Program for the Refinement of Crystal Structure*; University of Göttingen: Göttingen, Germany, 1997.
(40) Farrugia, L. J. *J. Appl. Crystallogr.* **1999**, *32*, 837.
(41) Drouza, C.; Keramidas, A. *J. Inorg. Biochem.* **2000**, *80*, 75.

Table 1. Crystal Data and Structure Refinement for Complexes **1**−**6**[a]

parameters	**1**	**2**	**3**	**4**	**5**	**6**
empirical formula	$C_{18}H_{44}N_8O_{21}V_2$	$C_{21}H_{36}N_8O_{16}V_2$	$C_{37}H_{68}N_{13}NaO_{35}V_4$	$C_{41}H_{95}N_{19}O_{40.5}V_4$	$C_{37}H_{68}KN_{13}NaO_{35}V_4$	$C_{17}H_{35}N_3Na_2O_{20.5}V_2$
cryst size (mm)	0.10 × 0.07 × 0.05	0.15 × 0.11 × 0.07	0.14 × 0.10 × 0.04	0.17 × 0.10 × 0.06	0.18 × 0.10 × 0.04	0.22 × 0.13 × 0.02
formula weight	810.49	758.46	1483.81	1740.39	1520.89	775.43
temperature	100(2) K	100(2) K	100(2) K	100(2) K	100(2) K	100(2) K
wavelength	0.71073 Å	0.71073 Å	0.71073 Å	0.71073 Å	0.71073 Å	0.71073 Å
cryst syst	triclinic	monoclinic	monoclinic	triclinic	monoclinic	orthorombic
space group	$P\bar{1}$	$C12/c$	$P12_1/n1$	$P\bar{1}$	$P12_1/n1$	$Pnaa$
a (Å)	10.571(2)	19.4212(9)	19.303(1)	14.0245(4)	18.2254(6)	12.2880(4)
b (Å)	13.559(2)	11.0769(5)	10.9657(5)	15.1826(5)	11.0201(4)	19.1695(6)
c (Å)	13.801(2)	29.339(1)	28.390(2)	19.6243(7)	31.007(1)	25.6802(9)
α (deg)	93.59(1)	90	90	94.517(3)	90	90
β (deg)	111.19(2)	98.816(3)	101.404(5)	101.466(3)	96.603(3)	90
γ (deg)	109.92(1)	90	90	107.133(3)	90	90
vol. (Å^3)	1694.7(5)	6237.0(5)	5890.7(5)	3871.2(2)	6186.3(4)	6049.1(3)
Z	2	8	4	2	4	8
ρ_{calcd} (Mg/m^3)	1.588	1.615	1.651	1.464	1.633	1.668
abscoeff (mm^{-1})	0.646	0.685	0.732	0.570	0.765	0.737
θ range for data collection (deg)	3.03 to 31.10	3.15 to 31.16	3.15 to 31.13	2.93 to 31.09	3.09 to 31.21	3.18 to 31.21
index ranges	$-15\le h\le 15$, $-18\le k\le 19$, $-19\le l\le 19$	$-27\le h\le 27$, $-15\le k\le 15$, $-42\le l\le 41$	$-26\le h\le 27$, $-15\le k\le 15$, $-40\le l\le 41$	$-20\le h\le 19$, $-22\le k\le 22$, $-28\le l\le 27$	$-26\le h\le 26$, $-15\le k\le 15$, $-44\le l\le 43$	$-17\le h\le 17$, $-27\le k\le 27$, $-35\le l\le 37$
collected	24636	38164	87133	85717	90475	87592
unique	9729	9293	18002	22650	18873	9514
R_{int}	0.0450	0.0210	0.0396	0.0359	0.0454	0.0421
data/parameters	18.50	20.60	21.40	22.74	21.82	18.80
max/min Δp (e Å^{-3})	1.081/−0.829	0.775/−0.706	1.326/−0.774	1.517/−1.014	1.639/−1.166	1.218/−0.534
final R indices (R, wR) [$I > 2\sigma(I)$]	0.0696, 0.1786	0.0432, 0.1190	0.0531, 0.1560	0.0558, 0.1780	0.0589, 0.1834	0.0512, 0.1513
R, wR (all data)	0.1136, 0.1899	0.0516, 0.1219	0.0920, 0.1663	0.0870, 0.1895	0.1032, 0.1931	0.0752, 0.1597

[a] Refinement method, full -matrix least-squares on F^2.

Scheme 1. Synthetic Routes of the Tetranuclear and Binuclear $V^{IV/V}$ Complexes

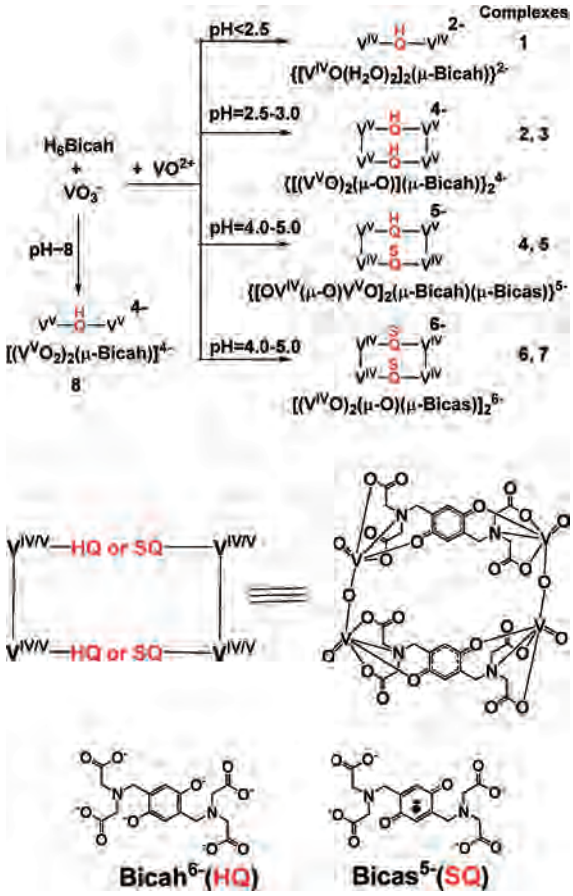

The counter ions are as follows: **1**, two guanidinium cations; **2**, four guanidinium cations; **3**, three qunidinium cations and one Na^+; **4**, five guanidinium cations; **5**, three guanidinium cations, one K^+· and one Na^-; **6**, two NH_4^+ and four Na^+; **7**, six Na^+; and **8**, four Na^+.

To stabilize the product from aerobic oxidation during isolation the solution was acidified and the neutral ligand H_6bicah was precipitated out.

The syntheses of the vanadium complexes are summarized in Scheme 1. When water solutions of equimolar quantities of AV^VO_3 [A = Na^+, K^+, guan$^+$, NH_4^+, the vanadium species in solution after dissolution of metavanadate salts are the vanadate monomer (VO_4^{3-}) dimer, tetramer, and pentamer and their protonated species], $V^{IV}OB$ (B = SO_4^{2-}, $2Cl^-$) and H_6bicah are mixed at various pHs in the range 2.5−5.0, crystals of the complexes **1**−**6** are obtained. These complexes differ from each other in the oxidation states of the vanadium atoms (IV or V) and the oxidation states of the ligand (*p*-hydroquinone and/or *p*-semiquinone). The type of the isolated complex is dependent on the pH and the counterions present in the solution. At pH below 3.0, the tetranuclear complexes **2** and **3** were isolated containing four V(V) atoms and two bicah^{6-} ligands. The total charge of the tetranuclear anion in these complexes is −4. At lower pHs, we also observed precipitation of crystals of the dinuclear complex **1** containing two V(IV) atoms and one bicah^{6-}. Two types of tetranuclear complexes were isolated at pH 4.5; one containing two V^{IV}, two V^V atoms, one bicas$^{\bullet 5-}$, and one bicah^{6-} (**4** and **5**) and the other four V^{IV} atoms and two bicas$^{\bullet 5-}$, (**6** and **7**,[31]). The HS^{5-} complexes were precipitated out of the solutions containing guan$^+$ or guan$^+$ together with K^+/Na^+, whereas the SS^{6-} only in the presence of Na^+ and/or NH_4^+ counterions. Rotating disk voltamograms of these solutions at pH range 4−5 (see discussion in the Electrochemistry section) show that 90% of the tetranuclear anions are in the SS^{6-} oxidation state. The EPR spectra of the aqueous solutions were not helpful because of the very broad peaks that diminish the resolution of the spectra. Better resolution was obtained in mixed solvent methanol/water solutions where both SS^{6-} and HS^{5-} were observed (Supporting Information, Figure S1).

The hydrolytic stability of the complexes in aqueous solutions was examined by measuring the absorption spectra for various concentration (6 μM−0.15 mM) and constant pH. The spectra obey Lambert−Beer's law at each pH (pH range from 3.0 to 4.5) indicating that the complexes are hydrolytically stable in solution.

X-ray Crystallography. The molecular structures of the anions of **1**−**6** are shown in Figure 1. Crystallographic data are provided in Table 1 and 2. Supporting Information, Tables S1−S6 contain the interatomic bond lengths and angles of **1**−**6**. The structures show two different nuclearity modes for the isolated molecules. Complex **1** is dinuclear with one μ-hydroquinonate ligand to bridge two V^{IV} atoms. The anions **2**−**6** are tetranuclear containing μ-hydroquinonate and/or μ-semiquinonate bridging ligands occupying the long sides of a rectangle and two V−O−V bridges defining the short sides of the rectangle. The vanadium atoms are in the oxidation state IV or V. The coordination environment around each vanadium atom in **1**−**6** is octahedral with one oxo group and the amine nitrogen of the tripod ligating group occupying the apical positions. Three oxygen atoms, originated from the two carboxylate and the hydroquinonate or semiquinonate groups of the tripod moiety, occupy the three out of the four equatorial positions of the octahedron. The fourth equatorial position is occupied by a water oxygen atom in complex **1** and by the bridging oxo group in complexes **2**−**6**.

Dinuclear Complexes. The structure of the dinuclear vanadium(IV) complex **1** is similar to the structure of the dinuclear vanadium(V) compound **8**[31] with the exception that an oxo group in **8** has been replaced by a water molecule [O(2)] in **1**. This results in the inevitable shortening of the V−O(4) bond length in **1** [1.997(3) Å] compared with that in **8** [2.209(3) Å] because of the weaker *trans* effect of the water donor oxygen than that of the oxo group. The rest of the bond lengths around vanadium ions are longer in **1** than in **8** with the most noticeable being the bond lengths between the vanadium atom and the hydroquinonate oxygen [V−O(3)], 1.951(3) and 1.952(3) Å for **1** and 1.864(3) Å for **8**. These values fall in the $V-O_{phenolate}$ length range reported for other V^{IV} and V^V phenolic complexes in the literature.[42–47]

It has been experimentally shown that the formal oxidation states of complexes containing non-innocent ligands can be reasonably established by examination of the $C-O_{phenolate}$ and the C−C bond lengths of the *o*-dioxolene ligands, which are strongly dependent on the formal charge of the

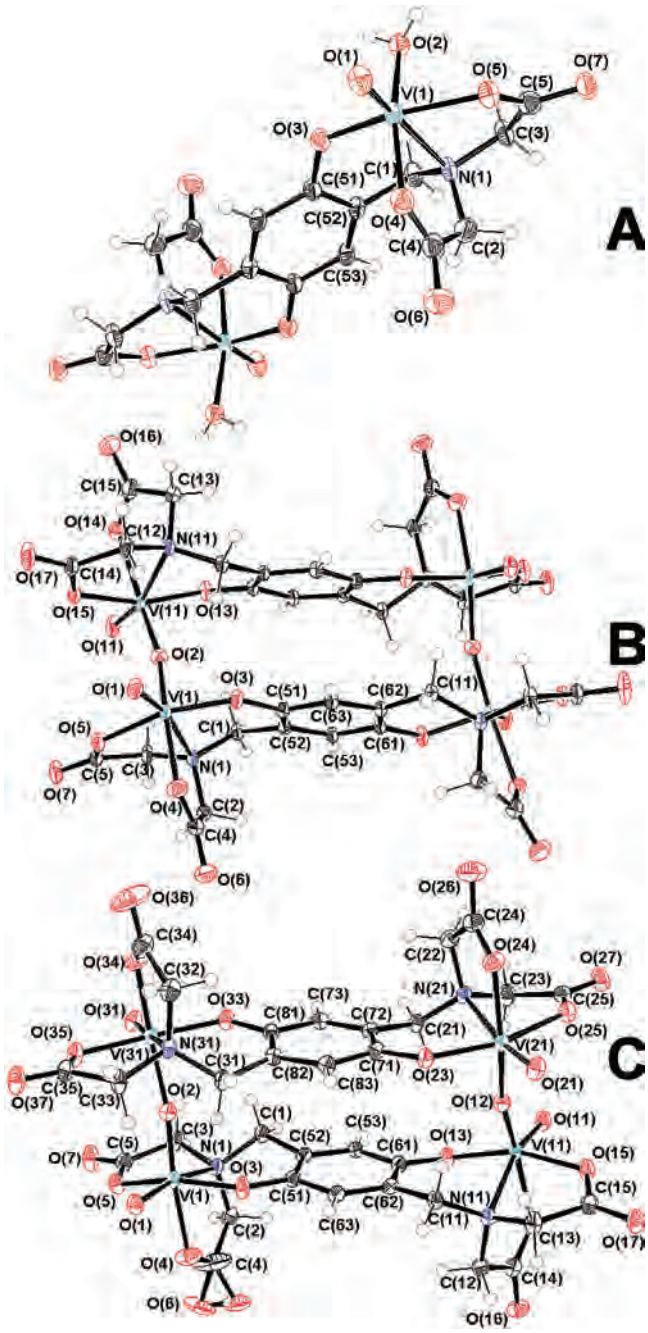

Figure 1. ORTEP (Oak Ridge Thermal Ellipsoid Plot) drawings of the anion of (A) **1**, (B) **2**, and (C) **4** at 50% probability ellipsoids giving the atomic numbering.

ligands.[21,25,26,48] In these molecules the C−$O_{phenolate}$ bond distance decreases from 1.35 Å in catecholate to 1.30 Å in *o*-semiquinonate and 1.23 Å in *o*-quinone species. The C−C bonds in catecholates are almost equidistant, because of the electron delocalization, with a mean value of 1.40 Å. In contrast, in the *o*-semiquinonate and *o*-quinone rings, the bonds are gradually becoming more localized with the longest bond to increase to 1.44 Å in *o*-semiquinonate and 1.50 Å in *o*-quinone species. Although the structurally characterized complexes of *p*-dioxolene ligands are fewer than those of the *o*- ones, the crystallographic data show that they follow a similar pattern. The $d_{C(n1)-O(HQ)}$ [$n = 5, 6$, where C(n1) refers to the carbon atom attached to the phenolate oxygen, numbering shown in Figure 1] [1.351(5) and 1.365(5) Å in **1** and 1.354(5) and 1.353(6) Å in **8**], as well the indistinguishable C−C interatomic bond distances in the aromatic ring, clearly show that the ligand in **1** and **8** is in the hydroquinonate oxidation state (Scheme 2a).

Tetranuclear Complexes. Although the anions **2**−**7** have the same rectangular structure, they differ from each other in the formal charges of both the complexes and the *p*-dioxolene ligands. The tetranuclear anions of **2** and **3** have a total charge of −4 which bear one and two electrons less than of **4**, **5** and of **6**, **7**, respectively. The anions of **2** and **3** contain two bridging ligated μ-bicah^{6-} ligands as it was clearly borne out by the observation that (i) the d_{C-C} are very close to each other with a mean value of 1.401 ± 0.014 Å and (ii) the $d_{C(n1)-O(hydroquinonate)}$ [$n = 5-8$, where C(n1) refers to the carbon atom attached to the phenolate oxygen, numbering shown in Figure 1] values of dioxolene ligand range from 1.335(3) to 1.346(3) Å which are long and typical for *p*-hydroquinonates.[49–54] In contrast, the anions of **6** and **7**[31] contain μ-bicas$^{\bullet 5-}$ π radical ligands;[54]the $C_{n1}-O_{SQ}$ bond lengths [1.315 (3), 1.320(3), and 1.322(5) Å] are shorter than the ones in **1** and **8** and longer than the bond length expected for quinone [∼1.26 Å],[55,56] and this denotes a partial double bond character (Scheme 2b). In addition, the C−C bonds of the six-membered ring (Table 2) exhibit a long−short−long pattern, as expected for *p*-semiquinonates. Although the six-membered ring of the ligated *p*-quinone ligands shows a similar pattern to *p*-semiquinonates, different bond lengths are expected [∼1.46, ∼1.33, and ∼1.46 Å][55,56] (Scheme 2c). Following the same reasoning, each of the anions of **4** and **5** were found to contain one bridging μ-bicas$^{\bullet 5-}$ π radical and one bridging μ-bicah^{6-}. Additional proof of our assignments is given by the similarities of the bond lengths of the *o*-dioxolene moieties in the catecholate and *o*-semiquinonate metal complexes with bicah^{6-} and bicas$^{\bullet 5-}$, respectively.[21,25,26,48]

(42) Schulz, D.; Weyhermuller, T.; Wieghardt, K.; Nuber, B. *Inorg. Chim. Acta* **1995**, *240*, 217.
(43) Dutta, S.; Basu, P.; Chakravorty, A. *Inorg. Chem.* **1993**, *32*, 5343.
(44) Schmidt, H.; Bashirpoor, M.; Rehder, D. *J. Chem. Soc., Dalton Trans.* **1996**, 3865.
(45) Maurya, M. R.; Kumar, A.; Bhat, A. R.; Azam, A.; Bader, C.; Rehder, D. *Inorg. Chem.* **2006**, *45*, 1260.
(46) Cornman, C. R.; Kampf, J.; Soo Lah, M.; Pecoraro, V. L. *Inorg. Chem.* **1992**, *31*, 2035.
(47) Cooper, S. R.; Koh, Y. B.; Raymond, K. N. *J. Am. Chem. Soc.* **1982**, *104*, 5092.
(48) Guetlich, P.; Dei, A. *Ang. Chem., Int. Ed. Eng.* **1997**, *36*, 2734.
(49) Foster, C. L.; Liu, X.; Kilner, C. A.; Thornton-Pett, M.; Halcrow, M. A. *J. Chem. Soc., Dalton Trans.* **2000**, 4563.
(50) Kunzel, A.; Sokolow, M.; Liu, F.; Roesky, H. W.; Noltemeyer, M.; Schmidt, H.; Uson, I. *J. Chem. Soc., Dalton Trans.* **1996**, 913.
(51) McQuillan, F. S.; Berridge, T. E.; Chen, H.; Hamor, T. A.; Jones, C. J. *Inorg. Chem.* **1998**, *37*, 4959.
(52) Calderazzo, F.; Englert, U.; Pampaloni, G.; Passarelli, V. *J. Chem. Soc., Dalton Trans.* **2001**, 2891.
(53) Sembiring, S.; Colbran, S. B.; Craig, D. C. *J. Chem. Soc., Dalton Trans.* **1999**, 1543.
(54) Chun, H.; Chaudhuri, P.; Weyhermuller, T.; Wieghardt, K. *Inorg. Chem.* **2002**, *41*, 790.
(55) Handa, M.; Mikuriya, M.; Sato, Y.; Kotera, T.; Nukada, R. *Bull. Chem. Soc. Jpn.* **1996**, *69*, 3483.
(56) Handa, M.; Matsumoto, H.; Naruma, T.; Nagaoka, T.; Kasuga, K.; Mikuriya, M.; Kotera, T.; Nukada, R. *Chem. Lett.* **1995**, 903.

Table 2. Comparison of Selected Chemical Bonds and Angles for Tetramer $V^{V/IV}$ Species and Δ Values

compound	V=O	V−(μ-O)	V−$O_{HQ/Q}$	V−(μ-O)−V	C−$O_{HQ/Q}$	C_{n1}−C_{n2}	C_{n2}−C_{n3}	C_{n1}−C_{n3}	Δ[a]
1[b]	1.601(3)	2.002(3)	1.950(3)		1.366(5)	1.401(6)	1.395(6)	1.393(5)	−1.94,HQ
	1.606(3)	2.009(3)	1.952(3)		1.353(5)	1.393(5)	1.393(5)	1.405(5)	−1.85,HQ
2	1.603(2)	1.840(2)	1.824(1)	166.10(9)	1.338(2)	1.413(3)	1.392(2)	1.415(2)	−1.67,HQ
	1.610(2)	1.748(2)	1.866(1)		1.346(2)	1.410(3)	1.391(2)	1.407(3)	
3	1.599(2)	1.818(2)	1.827(2)	178.8(1)	1.335(3)	1.405(4)	1.396(3)	1.400(4)	−1.75,HQ
	1.620(2)	1.729(2)	1.865(2)	166.9(1)	1.346(3)	1.414(4)	1.387(3)	1.395(4)	
	1.606(2)	1.875(2)	1.825(2)		1.327(3)	1.413(4)	1.385(3)	1.408(3)	−1.56,HQ
	1.613(2)	1.759(2)	1.878(2)		1.325(3)	1.421(4)	1.387(3)	1.405(3)	
4	1.622(2)	1.697(2)	1.878(2)	170.8(1)	1.346(3)	1.417(3)	1.388(4)	1.391(4)	−1.72,HQ
	1.625(2)	1.699(2)	1.879(2)	168.8(1)	1.352(3)	1.416(3)	1.391(4)	1.405(4)	
	1.597(2)	1.914(2)	1.880(2)		1.312(3)	1.432(3)	1.369(4)	1.412(4)	−1.30, SQ
	1.604(2)	1.934(2)	1.936(2)		1.309(3)	1.427(3)	1.386(4)	1.421(4)	
5	1.611(3)	1.707(3)	1.885(2)	169.5(2)	1.348(4)	1.417(5)	1.387(4)	1.400(5)	−1.70,HQ
	1.630(2)	1.699(2)	1.851(2)	175.0(1)	1.335(4)	1.407(5)	1.394(4)	1.404(5)	
	1.609(2)	1.926(2)	1.915(2)		1.299(4)	1.423(5)	1.375(5)	1.416(4)	−1.24, SQ
	1.607(3)	1.915(3)	1.903(2)		1.293(4)	1.433(5)	1.366(4)	1.399(5)	
6	1.616(2)	1.813(2)	1.867(2)	172.7(1)	1.321(3)	1.409(4)	1.371(4	1.406(4)	−1.38, SQ
	1.618(2)	1.809(2)	1.879(2)		1.313(3)	1.419(4)	1.369(4)	1.410(4)	
7[c]	1.620(3)	1.807(1)	1.886(3)	172.3(3)	1.322(5)	1.427(6)	1.371(6)	1.399(6)	−1.39, SQ
8[c]	1.652(3)	1.620(4)	1.864(3)		1.354(5)	1.386(6)	1.392(6)	1.381(6)	−2.02,HQ
	1.641(4)	1.626(4)	1.878(3)		1.353(6)	1.381(7)	1.384(7)	1.383(7)	−1.95,HQ

[a] The values of d_{1i} and d_{2i} for hydroquinone and *p*-quinone, respectively, are considered as the experimental bond lengths of the uncomplexed organic molecules.[59–65] The average values for C_{n1}−$O_{HQ/Q}$, C_{n1}−$C_{n2/n3}$ and C_{n2}−C_{n3} are 1.377 ± 0.004 Å, 1.385 ± 0.005 Å, and 1.384 ± 0.003 Å for the free hydroquinone and 1.266 ± 0.003 Å, 1.476 ± 0.002 Å, and 1.332 ± 0.005 for the free quinone [where C_{n1} refers to the carbon atom attached to the phenolate oxygen, $C_{n2/n3}$ refer to the rest of the aromatic carbons, numbering shown in Figure 1]. Δ values are the dioxolene charge calculated from eqs 1 and 2. [b] These bonds are referred to V^{IV}−O_{water} and they appear in double because in the asymmetric unit of **1** there two independent molecules. [c] From ref 31.

Scheme 2. Mean Values and Deviation from the Mean Values of the Bond Lengths in the (a) 1,4-Hydroquinonate and (b) 1,4-Semiquinonate Rings Calculated from the Crystal Structures of **1**−**8** and the (c) Reported Mean Values for 1,4-Quinone Rings[55,56]

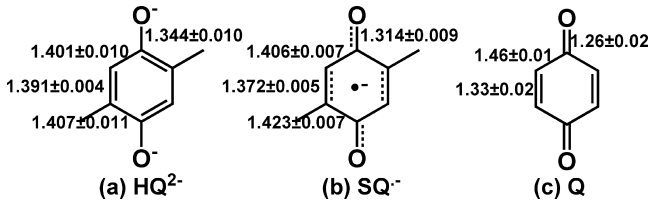

The characteristic quinoidal distortion upon oxidation allows the partial electron transfer to be quantitatively evaluated at each organic redox center of the tetranuclear complexes. The linear relationship of the charge of *o*-dioxolenes (Δ) versus the bond lengths of all the six intraring C/C ligand distances is given by the eqs 1 and 2[57,58] where d_i is the *i*th bond length of the dioxolene moiety under examination, and d_{1i} and d_{2i} are the *i*th bond lengths of the uncomplexed hydroquinone and *p*-quinone molecules,[59–65] respectively and *n* the number of the dioxolene bonds.

$$\Delta_i = -2(d_i - d_{2i})/(d_{1i} - d_{2i}) \quad (1)$$

$$\Delta = \left(\sum \Delta_i\right)/n \quad (2)$$

The results from the application of Δ statistical analysis on complexes **1**−**8** confirmed the oxidation state of the organic redox centers (Table 2). The Δ values deviate from the ideal values (0, −1, and −2 for quinone, semiquinonate, and hydroquinonate), with the largest deviation to be observed in one of the hydroquinones of complex **3**, (Δ = −1.56 instead of −2). These deviations are probably due to the coordination of the metal ion to the ligand and to the ionic interactions of the counter cations with the free carboxylate oxygen atoms of the tetranuclear anions which transfer charge from the organic ligands distorting further the structures of *p*-dioxolenes.[66] These data unambiguously define the oxidation level of the organic ligands in **2**−**7**, which render the four central metal ions as V^V in **2**, **3** and V^{IV} in **6**, **7**, whereas in **4**, **5** two vanadium ions are in the oxidation state V^V and two in V^{IV}.

The HS^{5-} in crystals of **4** and **5** do not possess crystallographically imposed symmetry. The mean length of the bonds around the two vanadium atoms coordinated to hydroquinonate (1.936 ± 0.004 Å) is smaller than that of the two vanadium atoms coordinated to semiquinonate species (1.965 ± 0.011 Å) indicating that the former atoms [V(1) and V(11)] are V^V and the latter [V(21) and V(31)] are V^{IV}. This is nicely corroborated with the fact that the V−O−V moiety is not symmetric. It contains short V^V−$O_{bridged}$ bonds ranging from 1.697(2) to 1.712(2) Å and long V^{IV}−$O_{bridged}$ bonds ranging from 1.910(2) to 1.934(2)

(57) Carugo, O.; Castellani, C. B.; Djinovic, K.; Rizzi, M. J. *J. Chem. Soc., Dalton Trans.* **1992**, 837.
(58) Drouza, C.; Keramidas, A. D. Charge Distribution in Vanadium *p*-(Hydro/Semi)Quinonate Complexes. In *Vanadium: The Versatile Metal*; Kustin, K., Pessoa, J. C., Crans, D. C., Eds.; ACS Symposium Series 974; American Chemical Society: Washington, DC, 2007; pp 352−363.
(59) Oswald, I. D. H.; Motherwell, W. D. S.; Parsons, S. *Acta Crystallogr., Sect. E: Struct. Rep. Online* **2004**, *60*, o1967.
(60) Arulsamy, N.; Bohie, D. S.; Butikofer, J. L.; Stephens, P. W.; Yee, G. T. *Chem. Commun.* **2004**, 1856.
(61) Patil, A. O.; Curtin, D. Y.; Paul, I. C. *J. Am. Chem. Soc.* **1984**, *106*, 4010.
(62) Pennington, W. T.; Patil, A. O.; Curtin, D. Y.; Paul, I. C. *J. Chem. Soc., Perkin Trans.* **1986**, *2*, 1693.
(63) Wallwork, S. C.; Powell, H. M. *J. Chem. Soc., Perkin Trans.* **1980**, *2*, 641.
(64) Bolte, M.; Margraf, G.; Lerner, W. *Cambridge Crystallographic Database* 2002.
(65) Sugiura, K.; Toyado, J.; Okamoto, H.; Okaniwa, K.; Mitani, T.; Kawamoto, A.; Tanaka, J.; Nakasuji, K. *Angew. Chem. Int. Ed. Engl.* **1992**, *31*, 852.
(66) McGarvey, B. R.; Ozarowski, A.; Tuck, D. G. *Inorg. Chem.* **1993**, *32*, 4474.

Å. In addition, the $V^{V}-O_{hydroquinonate}$ bond lengths [1.852(2)−1.885(2) Å] are slightly shorter than the respective $V^{IV}-O_{semiquinonate}$ bond lengths [1.880(2)−1.937(2) Å]. It is important to notice here that the $V^{IV}-O_{semiquinonate}$ bond distances are much shorter (1.89 Å mean value in **4**−**7**) than the bond distance of V^{IV} from phenolic oxygens (1.952 Å mean value in **1**) indicating the higher affinity of V^{IV} for the semiquinonate than the hydroquinonate oxygen donor atom.

Such localized structures have been observed for dinuclear mixed-valent V^{V}/V^{IV} species containing an asymmetric bent V−O−V bridge (angle less than 160°) and one or two π-donor ligands at the equatorial *xy*-plane (the short terminal V═O bond defines the *z*-axis).[42–44,67,68] On the other hand, σ-donor atoms at the equatorial plane result in the formation of mixed-valent V^{V}/V^{IV} complexes with delocalized valences containing symmetric and linear V−O−V bridges.[69–73] The tetranuclear anions **4** and **5** have almost linear V−O−V bridges at ∼170°, despite of the fact that the valences are localized at vanadium centers. Presumably, steric interactions in the rectangular structures do not permit further bending of the V−O−V bridges.

The bond distances and angles around each of the four vanadium atoms of **7** are equivalent. The asymmetric unit of **6** contains two different vanadium fragments. However, the bond lengths and angles of each fragment are indistinguishable or very close to each other. The V−O−V bridges are almost symmetric with the two $V-O_{bridged}$ bond distances at 1.814(2) and 1.807(1) Å. In contrast, the V−O−V bridges in **2** and **3** are not symmetric, with the short bonds ranging from 1.729(2) to 1.759(2) Å and the long ones from 1.818(2) to 1.875(2) Å. An opposite lengthening [1.865(2)−1.878(2) Å] and shortening [1.824(2)−1.827(2) Å] of the $V-O_{hydroquinonate}$ bonds keep the mean bond distances around vanadium atoms constant at 1.932 ± 0.004 Å. This behavior can be explained by the competition of the two π-donor oxygen atoms ($O_{hydroquinonate}$ and $O_{bridged}$) to form a π bond with the d_{xy} metal orbital.[42] Such a competition for the d_{xy} orbital is not observed for the V^{IV} complexes, **6** and **7**, because the d_{xy} orbital is half-filled and its antibonding character destabilizes the π bond.

The two benzene rings of the *p*-dioxolene ligands in **2**−**7** are nearly parallel to each other. The dihedral angle θ between the two planes, each defined by the six carbon atoms of each ring, for the HS^{5-} complexes **4** [2.58(9) °] and **5** [2.1(1)°] is larger than that of the SS^{6-} complexes **7** (0.000 °) and **6** [0.39(7) °]. Remarkably, θ is even larger at the HH^{4-} complexes **2** [6.41(7) °] and **3** [4.20(7) °]. The increment of θ at the hydroquinonate complexes is attributed to the steric factors in the tetranuclear cluster developed because of the inflexibility of the aromatic dioxolene ring. The benzene rings in these structures are significantly bent acquiring a convex curvature away from the center of the complex (Figure 2). The dihedral angle ϕ (Figure 2A) between the planes defined by the $C_{n1}-C$ bonds of the same ring, ranges from 1.5 to 2.0 ° for Hydroquinonate and 6.5 to 9.0 ° for semiquinonate rings. The planarity of the benzene ring reflects its aromaticity and thus, smaller ϕ angles are indicative of a better aromatic electron delocalization.[74] Apparently, the hydroquinonate are more rigid than semiquinonate rings and retain the planar aromatic character of the ring in the complexes. Strongly interacting π-planar dimeric charge-resonance organic complexes have been shown to exhibit a bending of the two components toward each other, whereas the distance between the two components is less than 3.5 Å.[75,76] The opposite bending observed here in addition to the long distance (from 3.5 to 3.7 Å) between the two arene moieties in the tetranuclear complexes indicates no significant electronic interaction between the two organic redox centers.

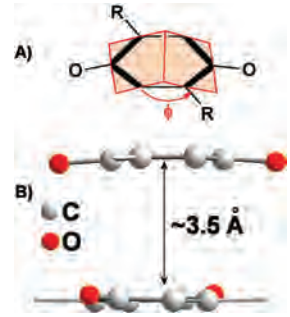

Figure 2. (A) Schematic depiction of angle ϕ between the two planes defined by $C_{n1}-C$ bonds. (B) Ball and stick drawing of the *p*-dioxolenes of the crystal structure of **6** showing the bending of the planar π-moieties.

Packing in the Crystal Structures. The highly negative charged anions, **1**−**6**, attract strongly the positive ions. The carboxylate oxygen atoms form extensive hydrogen bonds with the hydrogen atoms of water and $guan^{+}$ and/or ionic bonds with the Na^{+} or K^{+} counterions. The result is the creation of polymeric hydrogen and ionic bonded supramolecular 3D structures by self-assembly of the dinuclear or tetranuclear anions and the respective counterions. The stabilization of different redox tautomers depending on the counterions used in the synthesis of the tetranuclear anions suggests that these interactions might play an important role in the stabilization of the radicals, through charge transfer in solid state or in solution.

Complex **1** forms a 3D net with the threads to be constructed from the dinuclear anions connected together with the strong O(7)−H(2C) [1.78(5) Å] and O(17)−H(12C) [1.83(7) Å] hydrogen bonds. The hydrogen bonds O(3)−H(12D) [1.77(4) Å] and O(13)−H(2D) [1.79(4) Å] work as the glue

(67) Dutta, S. K.; Samanta, S.; Kumar, S. B.; Han, O. H.; Burckel, P.; Pinkerton, A. A.; Chaudhury, M. *Inorg. Chem.* **1999**, *38*, 1982.
(68) Dutta, S. K.; Kumar, S. B.; Bhattacharyya, S.; Tienink, E. R. T.; Chaudhury, M. *Inorg. Chem.* **1997**, *36*, 4954.
(69) Mahroof-Tahir, M.; Keramidas, A. D.; Goldfarb, R. B.; Anderson, O. P.; Miller, M. M.; Crans, D. C. *Inorg. Chem.* **1997**, *36*, 1657.
(70) Kojima, A.; Okazaki, K.; Ooi, S.; Saito, K. *Inorg. Chem.* **1983**, *22*, 1168.
(71) Nishizawa, M.; Hirotsu, K.; Ooi, S.; Saito, K. *J. Chem. Soc., Chem. Commun.* **1979**, 707.
(72) Launay, J.-P.; Jeanin, Y.; Daoudi, M. *Inorg. Chem.* **1985**, *24*, 1052.
(73) Holwerda, R. A.; Whittlesey, B. R.; Nilges, M. J. *Inorg. Chem.* **1998**, *37*, 64.
(74) Shishkin, O. V.; Omelchenko, I. V.; Krasovska, M. V.; Zubatyuk, R. I.; Gorb, L.; Leszczynski, J. *J. Mol. Struct.* **2006**, *791*, 158.
(75) Le Maqueres, P.; Lindeman, S. V.; Xochi, J. K. *J. Chem. Soc., Perkin Trans.* **2001**, 1180.
(76) Sun, D.-L.; Rosokha, S. V.; Linderman, S. V.; Kochi, J. K. *J. Am. Chem. Soc.* **2003**, *125*, 15950.

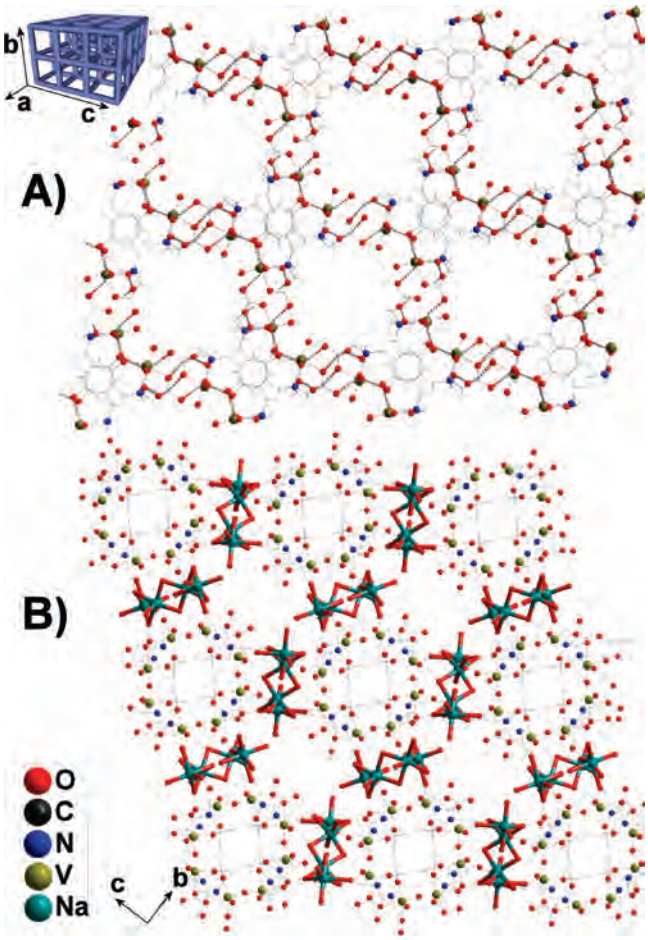

Figure 3. (A) Perspective view of the 3-D crystal structure of **1** viewed along the *a* axis depicting hydrogen bonds which connect the binuclear vanadium units generating a 3D net structure. Water and guan$^+$ counterions have been omitted revealing the rectangular shape spaces (~10 Å in diameter) of the net. (B) Perspective view of the 3-D crystal structure of **6** viewed along the *a* axis depicting ionic bonds between the Na^+ and the carboxylate oxygen atoms which connect the tetranuclear vanadium units generating a porous structure. Water and NH_4^+ counterions occupying the interspace have been omitted revealing one-dimensionally running channels of 11.387(2) Å diameter [distance between the Na(2) ions] and infinite length.

between the threads constructing the 3D net (Figure 3A). The rectangular shape spaces (~10 Å in diameter) between the net are filled with water and/or guan$^+$ counterions. In complex **3**, the three ionic bonds between Na(1) and O(26), O(17) and O(6) [2.338(3), 2.378(2), and 2.319(3), respectively] connect the tetranuclear anions, resulting in the formation of sheets parallel to axis *b*. These sheets are connected with hydrogen bonds through the guan$^+$ counterions. The most interesting 3D structure from among the rest of the tetranuclear complexes is that of **6**. Four sodium ions, two Na(1) and two Na(2), bridge together six tetranuclear units through the Na(1)−O(16) [2.458(3) Å], Na(1)−O(7) [2.425(3) Å], Na(2)−O(5) [2.492(2) Å], Na(2)−O(7) [2.546(3) Å], Na(2)−O(16) [2.353(3) Å], and Na(2)−O(17) [2.343(3) Å] ionic bonds. This bonding results in the formation of a porous 3D structure with the channels [11.387(2) Å diameter, distance between the Na(2) ions] having a direction parallel to axis *a* (Figure 3B). The channels are filled with water molecules and ammonium cations.

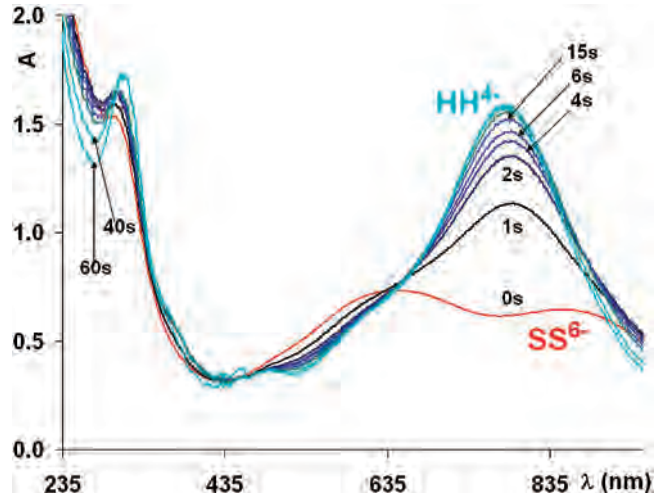

Figure 4. UV−vis electronic spectra of a 6.88 μM aqueous solution of **7** of constant ionic strength 0.1 M. The pH of the starting solution is 4.67, while at time equal to zero 34 μL of 1 M HCl (pH ~3.1) was added, and at certain time intervals, namely, 1, 2, 4, 6, 15, 40, 60 s, the electronic spectra (200−900 nm) were recorded.

UV−vis Spectroscopy. The UV−vis spectra of the HH^{4-} and SS^{6-} anions at pHs 3.1 and 4.7 are shown in Figure 4. The solid state reflectance UV−vis spectra exhibit the same peaks as the spectra of the compounds in solution showing that the complexes retain their structural integrity in solution (Supporting Information, Figure S2). The electronic spectrum of the dinuclear V^V complex **8** in aqueous solution exhibits a strong broad ligand-to-metal charge transfer (LMCT) band at 396 nm due to hydroquinonate→V(dπ) transition and a strong peak at 304 nm originated from the π-π* excitation of the hydroquinonate ligand.

All tetranuclear complexes, **2**−**7**, gave the same pH dependent spectra; thus, only the spectra of **7** will be discussed here at pHs 4.7 and 3.1. Examination of the spectra changes versus time shows that more than a half-hour is needed for this system to reach equilibrium after the pH had been adjusted from 4.7 to 3.1. However, the overlapped spectra (Figure 4) gave three isosbestic points in the range from 300 to 900 nm revealing that only the tetranuclear anions are participating in this reaction without any decomposition. The spectrum at pH above 4.5 exhibits two strong bands at 856 and 625 nm. On the basis of the intensity of the absorption (ε > 8000 M^{-1} cm^{-1}), we assign these strong transitions as LMCT semiquinonate→V(dπ) transfer excitations.[77–80] Intervalence transitions for the mixed-valent complex are also expected to appear in the visible-near IR region of the spectra; however, the intensity of those peaks is usually smaller, ε < 2000 $M^{-1}cm^{-1}$.[43,68,70] It is worth noticing that the peak at ~305 nm, originated from the π-π* transition of the phenols, is not present in the spectra indicating the oxidation of hydroquinonate to semiquinonate. At pH 3.0 the lower energy peak is shifted to higher energy

(77) Cornman, C. R.; Colpas, G. J.; Hoeschele, J. D.; Kampf, J.; Pecoraro, V. L. *J. Am. Chem. Soc.* **1992**, *114*, 9925.
(78) Hawkins, C. J.; Kabanos, T. A. *Inorg. Chem.* **1989**, *28*, 1084.
(79) Bulls, A. R.; Pippin, C. G.; Hahn, F. E.; Raymond, K. N. *J. Am. Chem. Soc.* **1990**, *112*, 2627.
(80) Cass, M. E.; Greene, D. L.; Buchanan, R. M.; Pierpont, C. G. *J. Am. Chem. Soc.* **1983**, *105*, 2680.

(from 856 to 780 nm), and the intensity is increased (23 000 $M^{-1}cm^{-1}$). This peak has been assigned as LMCT hydroquinonate→V(dπ) transfer excitations. The dramatic increase of the intensity covers the peak at 625 nm which now appeared as a shoulder at lower energy (642 nm). In addition, a new peak appeared at 317 nm, assigned to the π-π* transition of hydroquinonate, which confirms the reduction of semiquinonate to hydroquinonate in the solution at low pH.

The blue shift of the former LMCT band (856 nm → 780 nm) is attributed to the π-bonding between the empty d orbitals of V^V and the π orbitals of hydroquinonate which is stronger than the respective π-bonds of the half-filled d_{xy} orbital of V^{IV} and the π orbitals of semiquinonate ligand. This strong bonding will affect the electron accepting antibonding participating orbitals, having d metal character, by increasing their energy and consequently the LMCT energy. On the other hand, as evidenced by crystallography, the $V^V-O_{hydroquinonate}$ and $V^{IV}-O_{semiquinonate}$ bonds have similar strength, rendering that the $V^{IV}-O_{semiquinonate}$ is stronger σ-bonded than the $V^V-O_{hydroquinonate}$. Thus, the d antibonding orbital of V^V, which participates in the formation of the σ bond with hydroquinonate oxygen atom, lies at a lower energy than the respective orbital of V^{IV}−semiquinonate resulting in the red shift of the highest energy (625 → 642 nm) charge transfer band.

Magnetic Moments and NMR Spectroscopy. Complexes **4**, **5**, **6**, and **7** have effective magnetic moments 2.13, 2.15, 3.44, and 3.51 μ_B, respectively at 298 K which is less than the predicted spin-only values for three and six noninteracting one-electron paramagnetic centers (3.00 and 4.24 μ_B). The reduced magnetic moments in these complexes indicate an antiferromagnetic exchange interaction between the paramagnetic centers. Complexes **2**, **3**, and **8** are diamagnetic, and their ^{51}V NMR spectra at pH 3.0 (**2** and **3**) and 7.5 (**8**) gave one peak each, at −322 and −491 ppm (for HH^{4-} and **8**, respectively). On the basis of Rehder's[81] referencing scale one would predict similar chemical shifts for these complexes with the same donor atom set (NO_5) around vanadium atom. Pecoraro et.al[77] have proved that the magnitude of the ^{51}V NMR downfield shifts is correlated inversely with the LMCT energies of vanadium(V) complexes containing non-innocent ligands. This is in agreement with the observed values for HH^{4-} (−322 ppm, LMCT, 12800 cm^{-1}) and **8** (−491 ppm, 25250 cm^{-1}).

Electrochemistry. The redox properties of the ligand and complexes **2**−**8** were investigated by CV and rotating disk voltammetry (RD) in a pH range from 3.0 to 8.0. The CVs of **7** at various pHs are shown in Figure 5, and the data are collected in Table 3. The tetranuclear complexes **2**−**6** gave the same pH dependent CVs with **7**; thus, only the CVs of **7** will be discussed in detail.

The free ligand at pH = 3.1 gave one irreversible oxidation wave at $E_{pa} > 1.0$ V assigned to the oxidation of hydroquinone to *p*-quinone and a multielectron redox couple at −0.25 V ($E_{pc} - E_{pa} = 74$ mV) assigned to the reduction of the methylenaminodiacetic group (Supporting Information, Figure S3). These peaks are shifted to lower potential by increasing the pH. At pH = 4.6 the ligand shows a two electron peak originated from the oxidation of hydroquinone to quinone at 0.90 V (E_{pa}). The reverse cathodic scan gave two broad overlapping peaks at ∼0.2 V, associated with the oxidation of the ligand, assigned to the stepwise reduction of quinone to semiquinone and of semiquinone to hydroquinone. The reduction wave of methylenaminodiacetic at this pH has been shifted to more negative potentials, out of the redox limits of the solvent. The CV of **8** at pH = 6.9 exhibits one anodic peak at 0.93 V, and one very broad cathodic peak with maximum at 0.59 V appeared on the reverse cathodic scan originated from quinone-hydroquinone oxidation and reduction of the ligand, respectively.

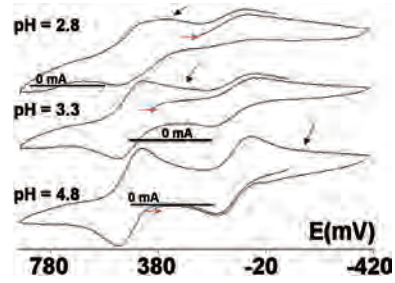

Figure 5. CVs of **7** (2.0 mM) in deoxygenated aqueous solution of 0.2 M KCl at 273 K recorded at pHs 2.8, 3.3, and 4.8. The shift of the semiquinonate−hydroquinonate wave to higher potentials up to 0.4 V is noted with an arrow while the pH is changed from the high to low values. The red arrows show the starting points of the CVs. A platinum disk and a platinum wire were used as working and auxiliary electrode, respectively. A $Hg/HgSO_4$ electrode was used as reference. The axis of potentials has been shifted so the values can be expressed versus NHE. The scan rate was 100 mV/sec.

Table 3. Electrochemical Data Obtained from the CVs of **7** at pHs 4.8 and 2.9

		E(V) vs NHE	
compound	process	E_a	E_c
SS^{6-} (pH = 4.8)	$SS^{6-} \rightleftharpoons HS^{5-}$	0.55	0.48
	semiquinonate→hydroquinonate	0.17	0.04
	semiquinonate→hydroquinonate	−0.03[a]	−0.28
	quinone→hydroquinonate	1.1	0.33[b]
HH^{4-} (pH = 2.8)	$SS^{6-} \rightleftharpoons HS^{5-}$	0.55	0.41
	$HS^{5-} \rightleftharpoons HH^{4-}$	0.45	0.31
		0.10	
	semiquinonate→hydroquinonate	0.88	0.33[b]
	quinone→hydroquinonate	1.1	0.42[b]

[a] This peak is associated to the cathodic peak. [b] These peaks are associated to the anodic peaks.

The CVs of **7** at pH 4.9 exhibit one reversible metal centered peak ($SS^{6-}-HS^{5-}$, eq 3) at 0.48 V. For electrochemically reversible processes, plots of *E* versus $RT \ln[(i_d - i)/i)]/F$ (*F*, faraday constant, *R*, gas constant) of the RDE voltammograms over a potential range between the quartile ($E_{1/4}$) and the three-quartile ($E_{3/4}$) potential values will be linear with intercept $E_{1/2}$ and slope $1/n$ (*n*, number of electrons).[82] The peak at 0.48 V meets these requirements with *n* equal to 1, for rotation speeds of 300, 500, and 1000 rpm. In addition, the $E_{1/2}$ value is essentially independent of the rotation speed, supporting the reversibility of the peak.

(81) Rehder, D.; Weidemann, C.; Duch, A.; Priebsch, W. *Inorg. Chem.* **1988**, *27*, 584.

(82) Bard, A. J.; Faulkner, L. R. In *Electrochemical Methods, Fundamentals and Applications*; Wiley: New York, 1980; (a) pp 160, 290; (b) p 288; (c) p 229.

Formation of HS^{5-} requires also a proton induced electron transfer from V^{IV} to semiquinonate group. In addition to the reversible metal centered wave, one quasi reversible ligand centered one electron redox couple appeared at 0.10 V. Careful examination of the voltammogram shows an additional broad cathodic wave at ~ -0.28 V and an associated anodic peak at ~ -0.03 V assigned to the reduction and reoxidation of the second semiquinone. The broadness of this peak indicates that the reduction of the semiquinones is associated to secondary decomposition reactions.

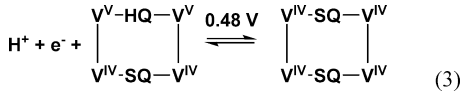

(3)

The oxidation of the ligand to quinone occurred at 1.1 V, and a cathodic peak appeared on the reverse scan for the reduction of quinone to semiquinone at 0.33 V. The ratio between the SS^{6-} and HS^{5-} tetranuclear anions was measured from the ratio of the anodic versus cathodic current of the reversible vanadium centered peak in the RD sweep voltammogram of **7** (Supporting Information, Figure S4). At pH = 4.5, 90% of the complex is in the SS^{6-} oxidation state in solution.

The pH of the solution of **7** was stepwise decreased from pH 4.5 to pH = 3.0, and the CVs were acquired at each step. These CVs showed a gradually shift of the broad semiquinone−hydroquinone wave to higher potentials up to 0.4 V and a change from broad irreversible peak to reversible couple, whereas the quasi-reversible peak at 0.10 V converted to an irreversible cathodic wave (Figure 5). The shift of the broad semiquinone peak shows that the semiquinones as expected are stronger oxidants at lower pH, favoring the electron transfer from the vanadium atoms to the ligand. The current at 0.6 V from anodic at pH 4.5 turned to 0 at pH 3.0 showing that all vanadium atoms have been oxidized to oxidation state 5+ (Figure 5, Supporting Information, Figure S4). The voltammograms of **2** and **7** at pH 3 were the same, confirming the oxidation of all vanadium atoms in solution. However, the two semiquinones are expected to oxidize two of the vanadium ions. Further oxidation of vanadium atoms has been attributed to oxidation from the atmospheric oxygen which was impossible to completely exclude from the aqueous solutions.

The final CV of **7** at pH 3.0 consisted of two one electron redox couples with $E_{1/2}$ 0.48 and 0.38 V (Figure 5) instead of one at pH 4.5. Both couples are assigned to metal redox processes associated with the related proton induced metal−ligand electron transfers described with eq 4 (SS^{6-}−HS^{5-}−HH^{4-}).

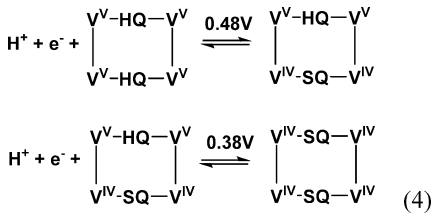

(4)

Two anodic peaks at 0.88 and 1.1 V are assigned to the oxidation of hydroquinone to semiquinone and of semiquinone to quinone, respectively. On the reversed scan the voltammogram showed two new cathodic waves at 0.42 V (reduction of quinone to semiquinone) and at 0.33 V (reduction of semiquinone to hydroquinone) associated with the oxidation processes of the ligand. These assignments were confirmed by acquiring cycles involving only the hydroquinone−semiquinone oxidation wave resulting in the disappearance of the quinone−semiquinone cathodic peak.

To confirm the above assignments, we performed exhaustive electrolysis of an aqueous solution of **7** at pH 4.5 and at constant potential of 0.60 V, whereas the speciation of the solution was concurrently monitored by UV−vis spectroscopy. The electrolysis was stopped at a current (*i*) equal to 5% of the initial current, and the total charge was found to correspond to two electrons per molecule oxidation. The pH of the final solution was 3.0, and the UV−vis spectrum was the same with that of HH^{4-}. Apparently, the SS^{6-} was stepwise oxidized to HS^{5-} and final to HH^{4-}. The H^+/redox association was further examined in solutions containing 0.1 M acetate buffer to maintain the pH stable during the electrochemical experiments. The CVs of these solutions (Supporting Information, Figure S5) gave peaks similar to those without buffer. The metal centered peaks seem to retain their reversibility in the buffered solution. However, exhaustive electrolysis of the buffered solution of **7** at pH 4.5 and at constant potential of 0.60 V gave a colorless solution indicating decomposition of the complex.

The reversibility of the metal centered peaks with and without the presence of buffer shows that the metal complexes retain their structure during the redox processes. The change of the pH from 4.5 to 3.0 results in an increment of the semiquinonate electron accepting ability oxidizing V^{IV} atoms to V^{V}. This increment is probably a result of the protonation of the semiquinonate/hydroquinonate oxygen atom. Similar protonation, as well as change of the redox potential, have been observed for *o*-dioxolene vanadium complexes with the protonation of the catecholate oxygen to increase the difficulty of the oxidation of catecholate to semiquinonate.[83,84] In addition, UV−vis spectroscopic titration of a solution of **7** gave a p*K* value 3.3 for the protonation of semiquinone which is very close to the p*K* (4.1) of the free *p*-semiquinone,[85] supporting further the mechanism.

Details on the H^+ Induced Redox Process and Biological Relevance. The pH induced transformation of SS^{6-} to HS^{5-} and HH^{4-} might occur through various mechanisms including disproportionation or decomposition of SS^{6-}, or valence tautomerism reaction accompanied with oxidation of the complex by strong oxidants such as atmospheric oxygen. The experimental data from the UV−vis spectroscopy (presence of isosbestic points), as well as the electrochemistry, indicate that neither the disproportionation nor the decomposition of the complex is occurring during the

(83) Baruah, B.; Das, S.; Chakravorty, A. *Inorg. Chem.* **2002**, *41*, 4502.
(84) Rath, S. P.; Rajak, K. K.; Chakravorty, A. *Inorg. Chem.* **1999**, *38*, 4376.
(85) Ilan, Y. A.; Czapski, G.; D, M. *Biochim. Biophys. Acta* **1976**, *430*, 209.

transformation. This was also confirmed by comparing the absorption of two equimolar aqueous solutions of HH^{4-} and of SS^{6-} at pH 3.0. Both solutions gave the same spectrum thus excluding the disproportionation or the decomposition of the complex as the main redox mechanism. Decomposition of the complex and formation of **1** in small quantities was observed at pHs less than 2.5. The change of the oxidation state of the ligand from semiquinone in the complexes isolated at pH 4.5 to hydroquinone in those at pH 3.0, as this was determined by crystallography, IR, and UV−vis spectroscopy, supports that the electron transfer of two electrons from two out of four V^{IV} ions to two semiquinone is one of the steps for the oxidation of two metal ions. However, this transfer cannot be accounted for by the oxidation of all four vanadium atoms.

To investigate if the atmospheric oxygen is the oxidant responsible for the oxidation of SS^{-6} to HS^{5-} and HH^{4-}, the recovery of SS^{6-} through a pH cycle (4.5→3.0→4.5) under argon and under atmospheric oxygen was determined by monitoring the changes of the UV−vis spectra of the solutions during the cycles. Although the experiment looks straightforward, it proved to be a difficult task mainly because of the difficulty of removing completely the oxygen from the aqueous solutions and the sensitivity of these compounds toward oxidation from the atmospheric oxygen. The UV−vis spectra, of carefully deoxygenated solution of SS^{6-} of constant ionic strength 0.1 M KCl for one pH cycles from pH 4.5 to 3.0 and backward, showed that in these conditions the electron transfer reaction is almost reversible by recovering ∼90% of the SS^{6-} species in each pH cycle (Supporting Information, Figure S6A,B). In contrast, under oxygen the spectra showed that almost half of the tetranuclear complex decomposes in each pH cycle (Supporting Information, Figure S6C). Apparently the reduction of HH^{4-} back to the SS^{6-} oxidation state at pH 4.5 consumes some of the ligand. Similar decomposition was observed for the solutions of HH^{4-} in which the pH increased from 3.0 to 4.5. These data show that the atmospheric oxygen oxidizes the complexes at low pH.

The oxidation of V^{IV} to V^{V} at pH 3 is unexpected if one considers that at low pHs the 4+ is the most stable oxidation state of vanadium in its aminocarboxylate and phenolaminocarboxylate complexes; thus, it is not expected to get oxidized from the atmospheric oxygen.[41,69,86,87] Apparently the V^{IV} should be oxidized to V^{V} by the semiquinonate and not by the atmospheric oxygen. This is also in accordance with the fact that the metal centers are oxidized only at pH 3.0 and not at pH 4.5 although the metal centered redox peak appeared at the same voltage at both pHs. Thus, the mechanism of the oxidation of the complexes at low pH should include first the formation of hydroquinonate valence tautomers and subsequent oxidation by the atmospheric oxygen.

In the CAOs at the intermediate reduced state (E_{red}) the reduced enzyme is oxidized by molecular oxygen to give hydrogen peroxide. The role of Cu^{+}/TPQ_{sq} in O_2 reduction has been a highly contentious issue. A few studies have shown that Cu^{+}/TPQ_{sq} is not actually required for the reaction with oxygen and that the Cu^{2+}/TPQ_{red} are the catalytically active species that react with O_2 converting TPQ_{red} to TPQ_{sq}.[13] Studies with model compounds have shown that TPQ_{red} readily undergo aerobic oxidation in the absence of metal ions suggesting that the redox partner may not be required for TPQ_{red} to react with O_2.[88] However, the mechanism in solution involves autoxidation leading to a radical chain reaction and so could be intrinsically different from the enzyme, where the cofactor cannot be freely diffused. Despite of the fact that our model contains vanadium instead of copper, it mimics very nicely this part of the catalysis mechanism of CAOs at several points. The equilibrium $Cu^{+}/TPQ_{sq}-Cu^{2+}/TPQ_{red}$ is analogous to the equilibrium between the $SS^{6-}-HS^{6-}-HH^{6-}$ species. The $pK_a = 3.4$ of $TPQ_{sq}H^{+}$ is in the pH region of the redox reaction observed for the tetranuclear vanadium complex. The SS^{6-} is stable toward atmospheric oxidation in analogy to the Cu^{+}/TPQ_{sq} which is not involved in the reaction pathway of O_2 reduction. On the other hand the HS^{6-} and HH^{6-} hydroquinone species are very reactive toward oxidation by O_2 showing similar behavior to Cu^{2+}/TPQ_{red}. Our results suggest that the reduced ligand is more susceptible to oxidation by O_2 than the semiquinone radical and that the metal ion does not participate directly in the reduction of O_2. According to our model, a possible role for the metal ions in the above metalloproteins is the stabilization of the organic radicals and the facilitation of the electron transfer for the recycling of phenol.

Conclusions

The complexation of metal ions with "non-innocent" ligands whose protonation modifies their redox properties is crucial for the synthesis of bistable systems with the pH controlling the intramolecular electron transfer between the metal and the ligand. Reaction of H_6bicah with vanadium(IV/V) precursors results in the synthesis of dinuclear and tetranuclear molecules exhibiting a pH controlled redox chemistry. Regulation of the redox properties of the ligand by varying the pH of the aqueous solutions of the tetranuclear complexes in a very narrow range (3.0−4.5) permitted for first time the isolation and crystallographic characterization of stable σ-bonded *p*-semiquinonate radical complexes in solid state and aqueous solution. The crystallographic results of this research clearly show that the paramagnetic V^{IV} nucleus has a higher affinity for the semiquinonate oxygen donor than for the hydroquinonate one. The strong $V^{IV}-O_{semiquinonate}$ σ-bond is considered as one of the reasons for the unexpected stabilization of the semiquinonate radical. The presence of the negatively charged carboxylate groups gives a high negative charge to the tetranuclear complexes, forcing strong interactions with counterions to take place, as this was found by crystallography, mimicking the environment of the phenol radicals in proteins. The selective crystallization of the various redox isomers depending on the type of counterions present in solution disclose the

(86) Crans, D. C.; Keramidas, A. D.; Amin, S. S.; Anderson, O. P.; Miller, S. M. *J. Chem. Soc., Dalton Trans.* **1997**, 2799.
(87) Crans, D. C.; Jiang, F.; Boukhobza, I.; Bodi, I.; Kiss, T. *Inorg. Chem.* **1999**, *38*, 3275.
(88) Mills, S. A.; Klinman, J. P. *J. Am. Chem. Soc.* **2000**, *122*, 9897.

significance of these interactions to the stabilization of the radicals. The spectroscopic study of the tetranuclear complexes in aqueous solutions in combination with the crystallographic characterization in solid state has shown an intramolecular pH induced electron transfer reaction between the ligand and the metal ion and the concurrent oxidation by the atmospheric O_2. Further investigation of the oxidation mechanism of these molecules is currently under way.

Acknowledgment. We thank the Research Promotion Foundation of Cyprus for the financial support of this work with the proposals ENTAX/0505/14, ENTAX/0504/8.

Supporting Information Available: Figure S1, the EPR spectrum of **7** (1.0 mM) in CH_3OH/H_2O 1:1 V/V solution. Figure S2, solid UV−vis reflectance spectra of **2**, **4**, and **7**. Figure S3, CVs H_6bicah. Figure S4, rotating disk voltammograms of **7**. Figure S5, CVs of complexes **2** and **7** at pHs 3.13 and 4.54, respectively, in deoxygenated aqueous solution containing buffer sodium acetate/acetic acid. Figure S6, (A) UV−vis spectra of **7** (6.5 μM) versus pH under argon atmosphere. Tables S1, S2, S3, S4, S5, and S6, selected bond lengths (Å) and angles (deg) for **1**, **2**, **3**, **4**, **5**, and **6**, respectively. This material is available free of charge via the Internet at http://pubs.acs.org.

IC800569T